Int J Mater Form (2018) 11:77–85
DOI 10.1007/s12289-016-1331-6

ORIGINAL RESEARCH

Research on the whole tool mesh reconstruction in the process of springback compensation for auto-body panels

Zhihui Gong[1,2] · Zhaobin Zhan[1] · Zhang Xu[3] · Guangyong Sun[1] · Gang Zheng[1] · Junjia Cui[1,2]

Received: 24 December 2015 / Accepted: 22 November 2016 / Published online: 6 December 2016

Abstract As an effective way to control springback, compensation technology is widely used in the field of automotive panel stamping. It is hard to reconstruct the whole tool mesh model containing addendum surface and binder surface in the compensation process, because the springback calculation is always carried out after trimming. A method for reconstructing the whole tool mesh automatically during springback compensation is proposed in this study. The method is based on the Displacement Adjustment (DA) compensation, and in the reconstructing process the blank mesh is split into two parts: the trimmed product and the addendum surface in trimming process. Base on this method, the changes of the reconstructed tool mesh can be avoided to ensure the accurate description of the tool surface. The reconstructed whole tool mesh can be used not only for the following stamping simulation but also for the springback compensation of automotive stamping parts.

Keywords Springback compensation · Stamping · Mesh stitching · Mesh mapping

✉ Junjia Cui
cuijunjia@hnu.edu.cn

[1] State Key Laboratory of Advanced Design and Manufacturing for Vehicle Body, Hunan University, Changsha 410082, China

[2] Key Laboratory of Advanced Manufacturing Technology for Automobile Parts, Chongqing University of Technology, Chongqing 400054, China

[3] College of Mechanical and Electrical Engineering, Hunan University of Science and Technology, Xiangtan 411100, China

Introduction

Springback is one of the most common defects in sheet stamping process, which causes the shape and size deviation from the design model, resulting in quality problems and assembly difficulties. It becomes the primary problem to be solved in the field of auto-body with the extensive use of high-strength steel and aluminum alloy. Several approaches have been employed to eliminate the springback [1–4]. Most of them focus on the variation of process parameters to increase the amount of plastic deformation, in order to reduce the ratio of elastic deformation. The advantage of these methods is that there is no need to modify the tool surface [5, 6]. Besides, two-step SHAPESET process or other process methods are also used to control the springback [1, 7–9], which also received a relatively large success to some extent. However, for high-strength steel components or other high strength new materials [10–12], it is difficult to entirely eliminate the springback effect due to large springback deformation.

Alternative springback compensation approach is tool compensation method. Within this method, the mold surface is premodified according to the numerical analysis, and makes the final product shape equal to the desired one in spite of large springback.

Tool compensation methods have been developed and improved by many researchers. Karafillis and Boyce [13] proposed the Force Descriptor Method (FDM), which compensates product by releasing the reversed inner stress with finite element (FE) simulation. However, this method suffers from lack of convergence for complicated parts [14]. Anagnostou et al. [15] improved the FDM by introducing compensation coefficient into the reversed inner stress and more accurate result was obtained. Cheng et al. [16] proposed an "accelerated springback compensation method" with the "springforward" moment, which made the convergence faster. The Displacement Adjustment (DA) Method proposed by Wagoner et al. [17] adjusted the nodes of

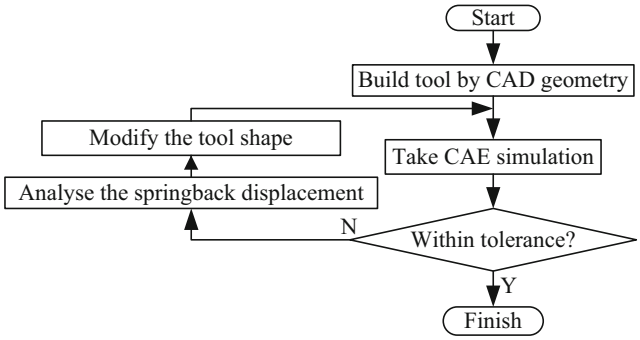

Fig. 1 Flow chart of the DA method

the product mesh with a geometric method to compensate the product, which is much easier and faster. The principle of the method is easy to understand and has been proven to be the most effective. The topological structure of the tool mesh is usually not consistent with the product mesh after forming. Therefore, Lingbeek et al. [18], Cafuta et al. [19] and Mole et al. [20] extended the DA method to obtain the compensated tool by considering the relations between product and tool geometry. On the basis of DA method, the comprehensive compensation (CC) method proposed by Yang and Ruan [21] was determined as the one that estimates the most appropriate compensation directions, in each iteration.

Generally, when the tool surface is modified, the springback displacement of the part becomes larger, therefore a coefficient called compensation coefficient is necessary to enhance the compensation. The compensation coefficient is usually defined as $\alpha = -1.0 \sim -2.5$ [18]. For one compensation, it is hard to determine the suitable compensation coefficient. But, for the iterative compensation, this compensation coefficient can be defined in a relatively large range, because it will only affect the convergence rate, not the final result. Iterative calculations are required to obtain the die compensation surface in each iteration. How to reconstruct the whole tool mesh model containing addendum surface and binder surface used for the next stamping simulation is one of the key issues that need to be solved in die design compensation process.

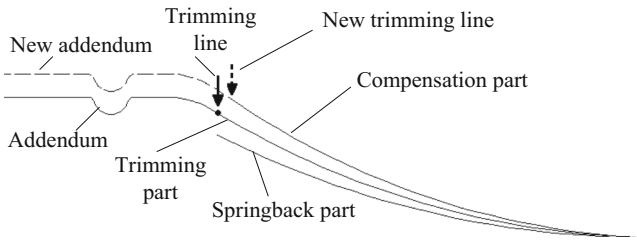

Fig. 3 Addendum in the springback compensation iteration

In this paper, a new reconstruction method of the whole tool mesh model is proposed and two problems are solved as follows: (1) Keep tool mesh precision in the iterative procedure; (2) Reconstruct the new addendum mesh for the next iteration. By solving these problems, the reconstruction tool mesh is obtained and can be used not only for the following stamping simulation but also for the springback compensation of automotive stamping parts.

Design compensation method

In general, springback displacement is different in various regions of stamping part with complex shape. In addition to CAE, there is no particularly effective way to predict springback. The DA method, which is based on CAE technology, is widely used for springback compensation. The flowchart of the DA is shown in Fig. 1. During DA method, the formed part mesh is compared with the springback mesh, and the springback displacement of each node is obtained. Thus, the compensation vector can be calculated by the springback displacement with compensation coefficient. Next, the compensation vectors are applied to the nodes of the forming part and the compensation model is finally obtained. According to the compensation model, the following stamping simulation can be carried out until the error attains a value within a reasonable range. Gan et al. [14] found that springback errors could be generally reduced more than 90% by three to four iterations. Therefore, the rate of DA method is relatively fast.

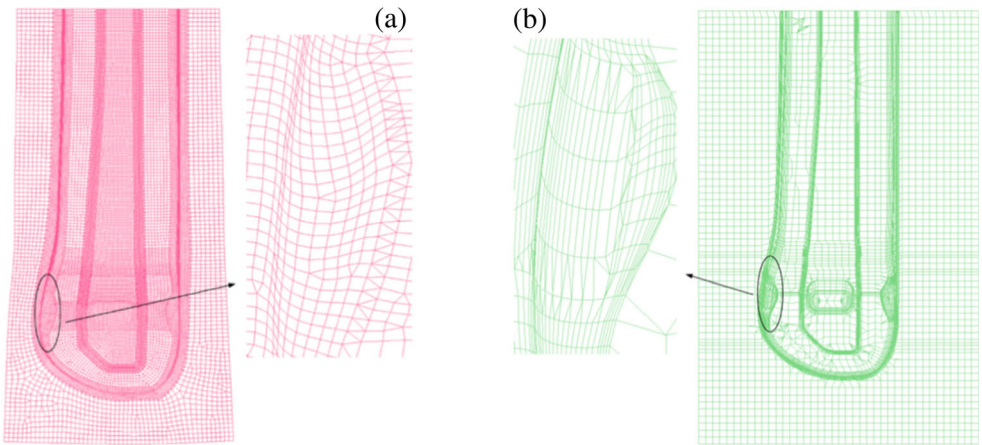

Fig. 2 Mesh topology used in the DA method for the stamped blank mesh and tool mesh: **a** stamped blank; **b** tool

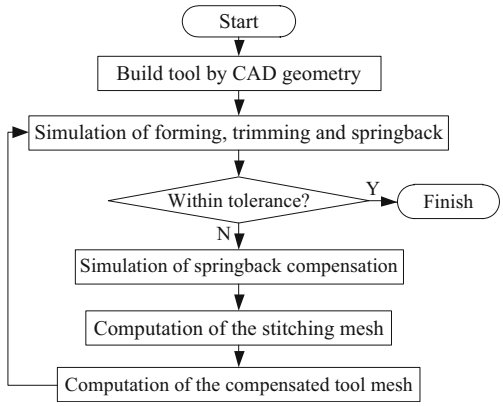

Fig. 4 The flowchart of the stitching compensation method

Generally, the tool (punch or die) mesh in the following iteration is replaced by the compensated blank mesh. However, the mesh size of the blank and the tool are different, since different rules apply to the mesh generation method. Compared with the blank mesh, the mesh of the tool is finer on the small features as shown in Fig. 2, which means it is more suitable for stamping simulation. Therefore, it is beneficial to keep the topology of the tool mesh unchangeable during the iterative compensation procedure.

For deep drawing auto-body panels, springback simulation should be always carried out after trimming. The addendum part, which is activated in the following iteration simulation, is not contained in the mesh after springback compensation, as shown in Fig. 3. Therefore, in order to improve the accuracy

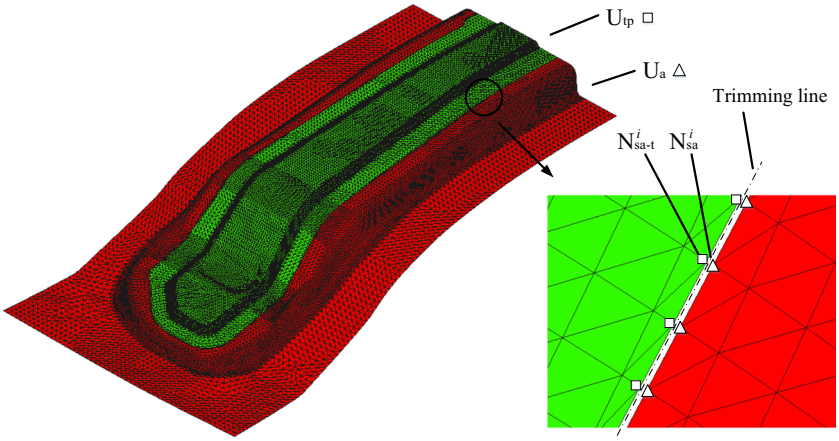

Fig. 5 The one-to-one correspondence relationship in the boundary of addendum mesh and product mesh

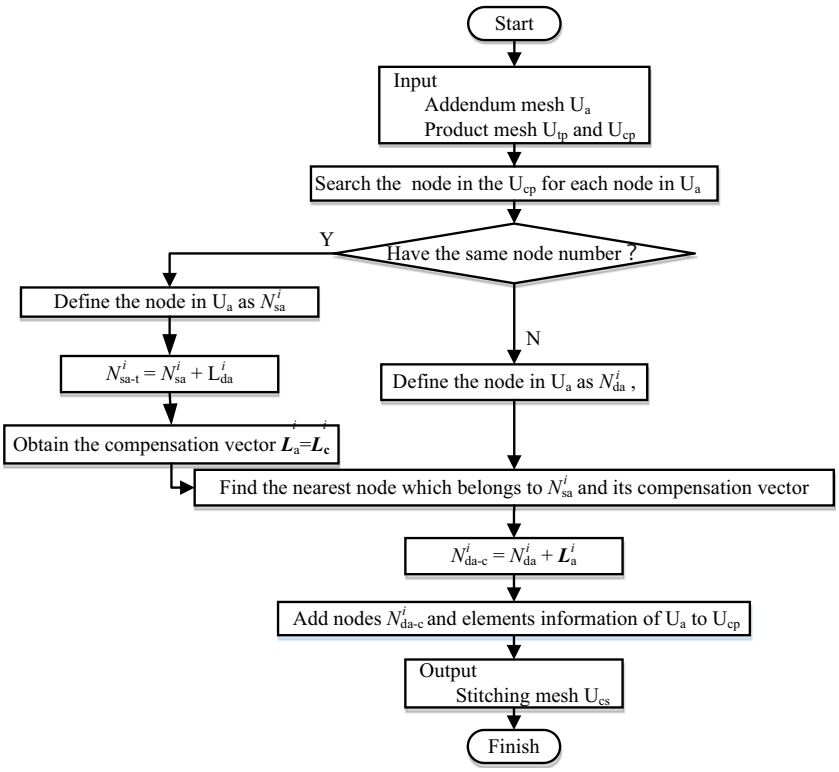

Fig. 6 Flowchart of the generation of the stitching mesh U_{cs}

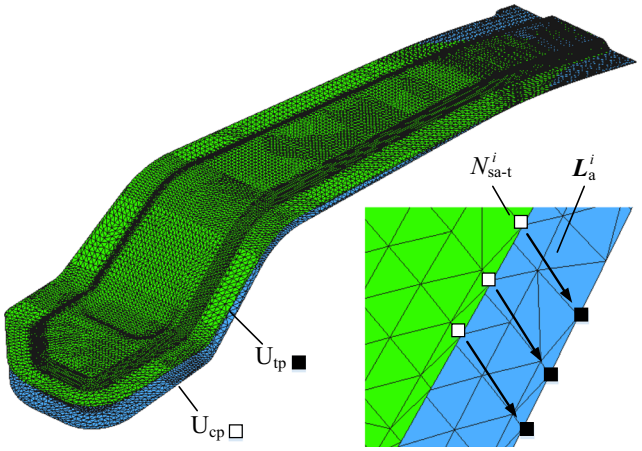

Fig. 7 Computation of the addendum compensation vectors L^i_a

of springback calculation, the addendum part should also be considered in the reconstruction process, used in the iterative procedure.

The stitching compensation method

To solve the problems above, a new method called "stitching compensation method" is proposed. In this method, the addendum part is also included to be used to generate the whole tool mesh and the shape of addendum, especially when the binder is unchanged in the iterative procedure. By moving the nodes of the tool mesh, the previous addendum mesh trimmed results can be used for the reconstruction of the whole tool mesh in the next stamping simulation. In the stitching compensation method, first a compensated stitching mesh is produced from the formed part mesh, considering also the part that was trimmed. However, since this mesh has the same topology of the blank, in a second step the compensated tool mesh is changed, based on the information stored in the compensated stitching mesh. According to the relations between the tool and the stitching mesh, the springback compensation tool is obtained by adjusting the nodes of the tool mesh. The procedure of the stitching compensation is shown in Fig. 4.

Springback compensation simulation

At the beginning of the procedure, the FE model is obtained using the tool geometry (U_t) defined in the design process. Forming (U_{ts}), trimming (U_{tp}) and springback (U_{sp}) processes are simulated by the CAE software. The U_{ts}, U_{tp} and U_{sp} are used to specify the product mesh at the end for forming, after the trimming and after springback, respectively. The springback vectors L^i_s can be calculated by:

$$L^i_s = N^i_{sp}(x,y,z) - N^i_{tp}(x,y,z) \quad (1)$$

Where i is the node number which is defined in the mesh generation process; x, y and z are the coordinate values, respectively. The coordinates of the nodes of the compensated product mesh N^i_{cp} are modified by the product compensation

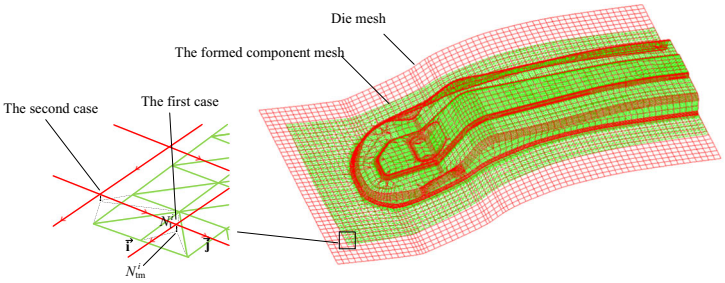

(a) The mesh mapping methods

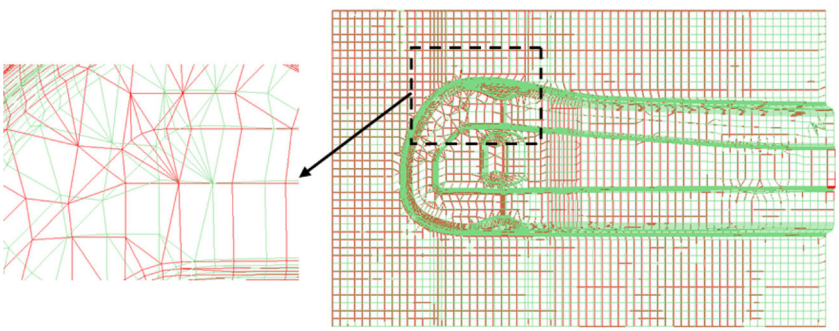

(b) Meshes of the tool and the blank

Fig. 8 Two cases in the mapping process

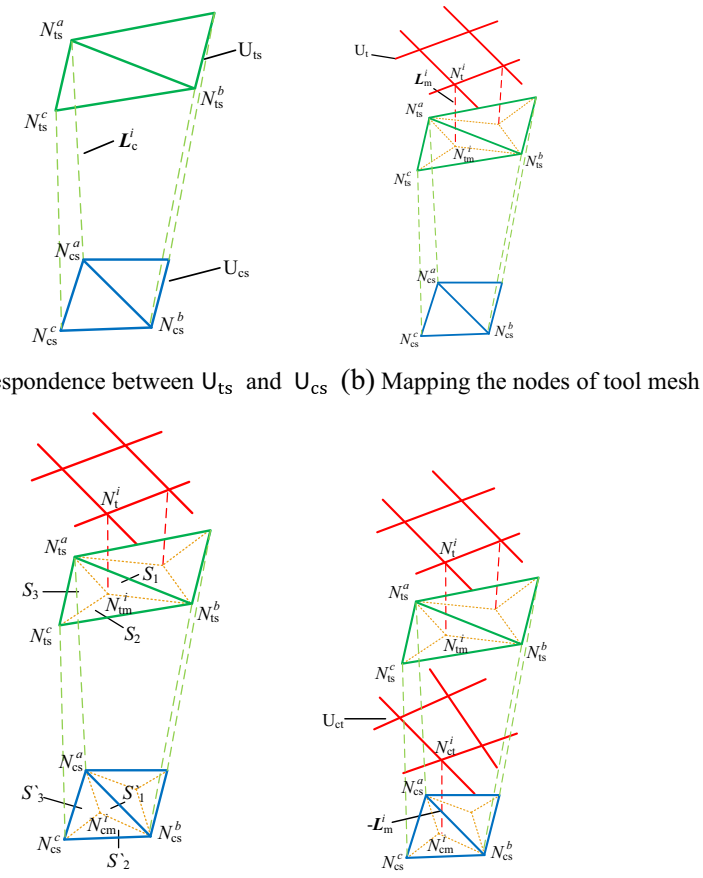

Fig. 9 The process of obtaining the main compensated tool mesh

(a) The correspondence between U_{ts} and U_{cs} (b) Mapping the nodes of tool mesh

(c) The element shape function (d) Computation of the nodes N_{ct}^i

vectors $\boldsymbol{L}_c^i$, which are related to the springback vectors $\boldsymbol{L}_s^i$, as shown in:

$$\boldsymbol{L}_c^i = \boldsymbol{L}_s^i \cdot \alpha \tag{2}$$

Where α is the compensation coefficient which is defined before the springback compensation. The coordinates of the nodes of the compensated product mesh N_{cp}^i can be calculated by:

$$N_{cp}^i(x,y,z) = N_{tp}^i(x,y,z) + \boldsymbol{L}_c^i \tag{3}$$

The stitching mesh computation

The previous step allows the definition of the compensated product mesh (U_{cp}), which does not contains the part that was removed by the trimming operation. After springback compensation, the boundary lines of the compensated product mesh (U_{cp}) are different from that of the trimmed mesh (U_{tp}). If the mesh is not subdivided in the trimming operation, the nodes located on the trimming boundary of the compensated product mesh and the addendum mesh (U_a), have one-to-one correspondence relationship (such as the same node number), as shown in Fig. 5. This figure shows that the nodes and connectivity of the product mesh (U_t) are stored in the trimming part (U_{tp}) and the addendum part (U_a).

According to this relationship, the addendum mesh and the compensated product mesh can be stitched. The flowchart of this procedure is shown in Fig. 6 and all the nodes of addendum mesh are adjusted. The nodes of the addendum mesh N_a^i are divided into N_{sa}^i and N_{da}^i based on their relationship with the trimming mesh node numbers. The N_{sa}^i are the addendum nodes that present a one-to-one correspondence with the trimming boundary nodes N_{sa-t}^i of the product mesh. Therefore,

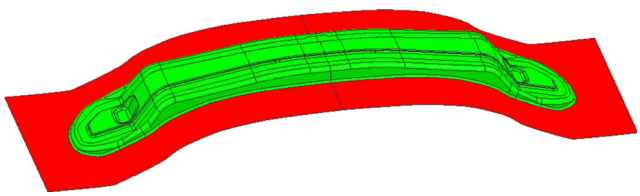

Fig. 10 The front cabin beam digital model

Table 1 The mechanical property parameters of DP500 steel blanks

t(mm)	E (GPa)	n	k(MPa)
1.2	207	0.2	802

Table 2 The stamping process parameters

Binder force (kN)	Drawbead restrain force (kN)	Punch velocity (mm/s)	Blank holder closing velocity (mm/s)
285	0.14	5000	2000

Fig. 11 The illumination map of original die mesh

for each N^i_{sa} node, the compensation vector $\boldsymbol{L}^i_a$ is actually the same as the compensation vector $\boldsymbol{L}^i_c$ determined in the previous step (as shown in Fig. 7). The nodes N^i_{da} present no direct correspondence. Thus, it is necessary to search for the nearest node, which belongs to the N^i_{sa} set. The compensation addendum node N^i_{da-c} is obtained using the compensation vector $\boldsymbol{L}^i_a$ of the nearest node, as shown in Eqs. (4) and (5). Combining the positions information of N^i_{da-c} and N^i_{cp}, stitching mesh U_{cs} can be obtained by synthesizing the elements information of addendum mesh U_a and compensated product mesh U_{cp}.

$$\boldsymbol{L}^i_a = \boldsymbol{L}^i_c \tag{4}$$

$$N^i_{da-c}(x,y,z) = N^i_{da}(x,y,z) + \boldsymbol{L}^i_a \tag{5}$$

The compensated tool mesh computation

The nodes of original tool mesh U_t are mapped onto the formed product mesh (U_{ts}), such that the mapping vectors m are normal to the finite element of the Uts mesh. There are two cases in the mapping processes (as shown in Fig. 8 (a)): (1) the mapping nodes are inside the elements or on the edges of elements, (2) the mapping nodes are outside the elements. Most of the tool mesh nodes belong to the first case and only a small number of nodes located in the binder part belong to the second case. Figure 8(b) shows the meshes of the tool and the blank after the mapping process. The tool mesh is offset by a certain angle in order to enable the observation of the mesh morphology. Because the tool mesh is directly obtained through the mapping process of the formed blank mesh, it can be seen that the node coordinates of the tool mesh coincides with that of the formed blank. It can be seen that the tool mesh is the same to the blank mesh. The node coordinates of the tool mesh coincides with that of the blank. The tool mesh is offset by the certain angle in order to observe the mesh morphology.

For the first case, the nodes of the tool mesh are compensated as shown in Fig. 9. For each node of the tool mesh N^i_t, a search is performed to identify the nearest element of the formed blank mesh U_{ts}, to enable its vertical mapping onto this element (Fig. 9(b)). This allows obtaining the coordinates of the mapping nodes N^i_{tm}. The mapping vectors $\boldsymbol{L}^i_m$ are computed as:

$$\boldsymbol{L}^i_m = N^i_t(x,y,z) - N^i_{tm}(x,y,z) \tag{6}$$

According to the stitching mesh computation, U_{ts} and U_{cs} have the same mesh topology and the same node number, as shown in Fig. 9(a). The element shape function:

$$S_1 : S_2 : S_3 = S`_1 : S`_2 : S`_3 \tag{7}$$

Where S_1, S_2 and S_3 are the areas of $\Delta N^a_{ts} N^b_{ts} N^i_{tm}$, $\Delta N^b_{ts} N^c_{ts} N^i_{tm}$ and $\Delta N^a_{ts} N^c_{ts} N^i_{tm}$, respectively. $S`_1$, $S`_2$ and $S`_3$ are the areas of $\Delta N^a_{cs} N^b_{cs} N^i_{cm}$, $\Delta N^b_{cs} N^c_{cs} N^i_{cm}$ and $\Delta N^a_{cs} N^c_{cs} N^i_{cm}$, respectively. a, b, c are the node numbers, respectively. Only parameter N^i_{cm} is unknown in the Eq. (7).

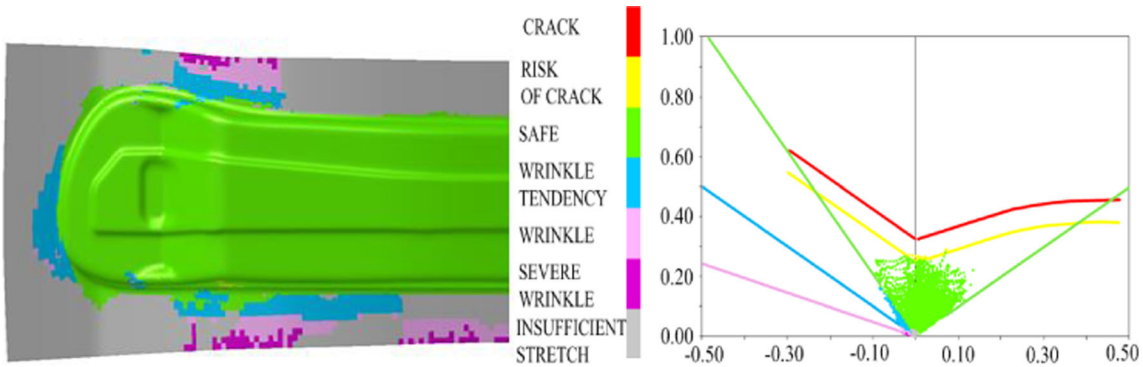

Fig. 12 Forming simulation result in the first CAE simulation

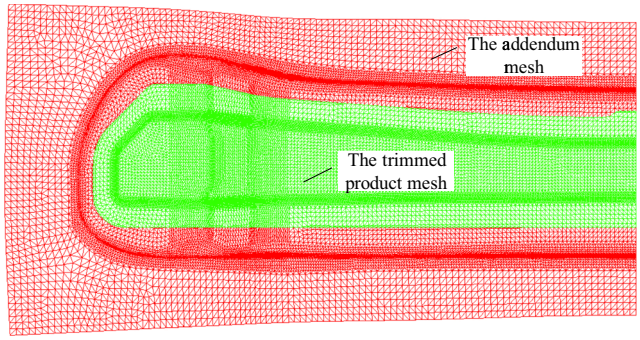

Fig. 13 Trimmed product mesh and addendum mesh

Fig. 15 The illumination map of compensated die mesh

Consequently, the compensated mapping node N^i_{cm} can be calculated.

The nodes of the compensated tool mesh N^i_{ct} can finally be achieved by applying the vectors $-\boldsymbol{L}^i_m$ to the nodes N^i_{cm}, as shown in Fig. 9(d). The tool compensation vectors $\boldsymbol{L}^i_{tc}$ of the nodes in the first case are computed as.

$$\boldsymbol{L}^i_{tc} = N^i_{ct}(x,y,z) - N^i_t(x,y,z) \tag{8}$$

For the second case, all nodes which are located in the binder part and the shape of binder part mesh have fewer changes in the springback compensation. The compensation vector for each node is equal to the tool compensation vector $\boldsymbol{L}^i_{tc}$ obtained for the nearest node that fulfills the conditions of the first case. So the tool nodes for the second case are compensated by the corresponding compensation vector.

Replacing all nodes of the original tool mesh with the compensated nodes, the compensated tool mesh U_{ct} is obtained. Only node positions are adjusted in the tool compensation. The compensated tool mesh U_{ct} has the same topology to the original tool mesh U_t. Consequently, the compensated tool mesh is suitable for the stamping process.

Numerical simulation

The front cross member of a car is analyzed with the method proposed in the previous sections. Figure 10 shows the geometry model for stamping simulation. Only half of the tool and blank is used for simulation due to symmetry conditions. This simulation mainly aims to test the proposed stitching compensation method. Consequently, the whole tool mesh is compensated in one iteration.

The as-received material is a DP500 steel and the blank has the dimension of 310 × 618 × 1.2 mm. The mechanical property parameters are listed in the Table 1, in which t is the blank thickness, E is the elastic modulus, n is the hardening exponent and k is the hardening coefficient. The stamping process parameters are shown in Table 2.

Firstly, it is necessary to obtain the compensated product mesh. The original die is meshed before the stamping simulation, as shown in Fig. 11. The forming process simulation is carried out with dynamic explicit analysis, and the simulation results are shown in Fig. 12. Secondly, the trimming simulation without mesh subdivision is executed to get the trimmed product mesh and addendum mesh, as shown in Fig. 13. Thirdly, springback simulation is performed with static implicit analysis, the simulation results are compared with the designed product and the error is shown in Fig. 14. The figure shows that the maximum error is 16.615 mm, which is beyond the allowable error. Consequently, the DA method is used to performed the springback compensation and obtain the compensated product mesh. The springback compensation coefficient α is set to be −1.2. Finally, addendum mesh and compensated product mesh are stitched to get the compensated stitched mesh. The trimmed stitched mesh corresponds to the formed component mesh. is obtained by the addendum mesh and trimmed product mesh.

The addendum mesh and the compensated product mesh are stitched to get the compensated stitched mesh. The original die mesh is compensated according to the relationship between the tool mesh and blank mesh. The nodes of the original die mesh

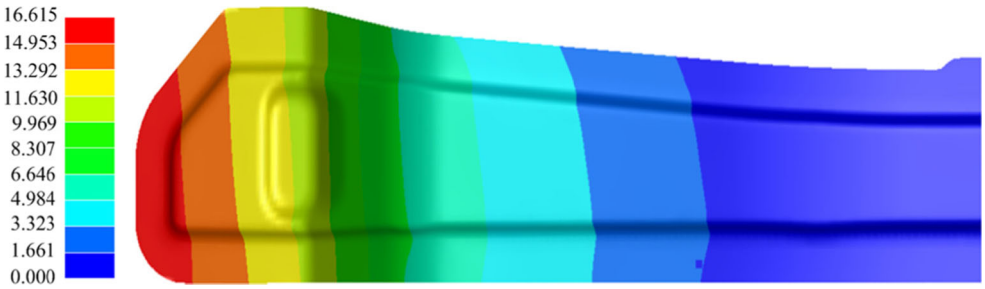

Fig. 14 Product shape errors in the first springback simulation

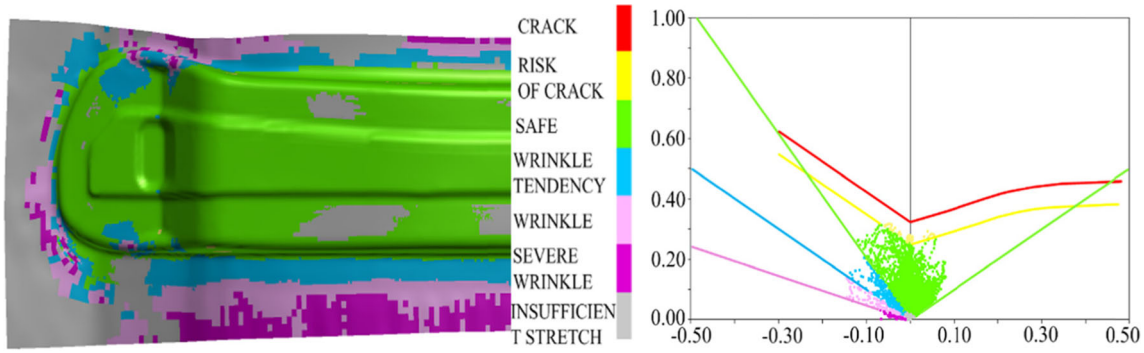

Fig. 16 Forming simulation result in the second CAE simulation

Fig. 17 Part shape errors in the second CAE simulation

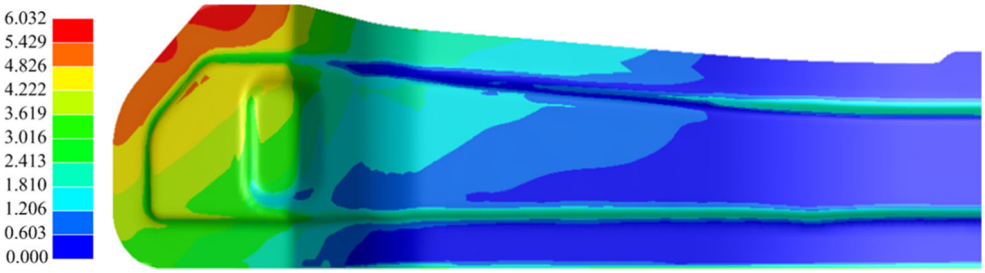

are mapped to the trimmed stitching mesh, and the mapping vectors are determined by the Eq. (6). There are 7707 nodes of die mesh in total. Among these nodes, 6419 nodes are mapped in the formed component mesh and 1288 nodes are outside this mesh. So 6419 nodes are compensated in the first mapping process and 1288 nodes are compensated in the second mapping process. The whole compensated die mesh is acquired after the original die nodes are compensated, as shown in Fig. 15.

The other CAR simulation is carried out to verify the compensated die mesh. The corresponding mesh of the punch and the binder is obtained by offsetting the whole compensated die mesh. The original process parameters are the same as in the first simulation. It can be seen from the Fig. 16 that the surface of the product part is perfectly formed. The final product shape is obtained after the trimming and springback simulation. Figure 17 shows the errors between the final product and the designed product. Compared with maximum product shape error in the first simulation (16.615 mm), the error value (6.074 mm) in the second simulation is reduced by 63.4%. The present error basically meets the requirement of designed compensation.

In this work, the correctness and effectiveness of the proposed springback compensation method is not fully verified by experiments. Further studies considering the experimental verification of complex shape parts are recommended.

Conclusions

In this paper, the stitching compensation method is proposed to compensate the tool mesh by adjusting the nodes positions. The potential of this method is tested through CAE simulations of a complex part. The main conclusions can be drawn as follows.

1) The addendum mesh is compensated by the proposed stitching compensation algorithm. This method can significantly decrease the workload and the addendum mesh keeps the original shape.
2) The node topology of the tool mesh remains unchanged during the compensation process. This method does not only ensure the accuracy of the tool, but also contributes to the improved convergence of the compensation procedure.
3) The proposed stitching compensation method is tested through the CAE analysis of a car front cross member, demonstrating that the compensation algorithm is efficient and practical.

Acknowledgements The authors would like to acknowledge the project supported by the National Natural Science Foundation of China (Grant No. 51475155, 51405149) and National Science and Technology Major Project of the Ministry of Science and Technology of China (Grant No. 2014ZX04015051).

Compliance with ethical standards

Conflict of interest statement None

References

1. Ayres RA (1984) SHAPESET: a process to reduce sidewall curl springback in high-strength steels rails. J Appl Meteorol 3:127–134

2. Hassan H, Maqbool F, Güner A, Hartmaier A, Khalifa NB, Tekkaya AE (2016) Springback prediction and reduction in deep drawing under influence of unloading modulus degradation. Int J Mater Form 9:619–633
3. Raghavan B, Quilliec GL, Breitkonpf P, Rassineux A, Roelandt JM, Villon P (2014) Numerical assessment of springback for the deep drawing process by level set interpolation using shape manifolds. Int J Mater Form 7:487–501
4. Chatti S, Fathallah R (2014) A study of the variations in elastic modulus and its effect on springback prediction. Int J Mater Form 7:19–29
5. Sunseri M, Cao J, Karafillis AP, Boyce MC (1996) Accommodation of springback error in channel forming using active binder force control: numerical simulations and experiments. Trans ASME 118: 426–435
6. Liu YC (1988) The effect of the restraining force on shape deviations in flanged channels. J Eng Mater Technol ASME 110:389–394
7. Li G, Hu JN, Zhang XK, Hu P (2008) Springback characteristics and control technology of the forming sheet. [J]-Automob Technol α Material 6:15–18
8. Schmocket D, Beth M (1993) Springback reduction in drawbending process of sheet metals. CIRP Ann Manuf Technol 42(1): 339–342
9. Moon YH, Kang SS, Cho JR, Kim TG (2003) Effect of tool temperature on the reduction of the springback of aluminum sheets. J Mater Process Technol 132(1):365–368
10. Li G, Liu YQ, Du T, Tong HL (2014) Algorithm research and system development on geometrical springback compensation system for advanced high-strength steel parts. Int J Adv Manuf Technol 70(1):413–427
11. Fiorotto M, Lucchetta G (2013) Experimental investigation of a new hybrid molding process to manufacture high- performance composites. Int J Mater Form 6:179–185
12. Badr OM, Rolfe B, Hodgson P, Veiss M (2015) Forming of high strength titanium sheet at room temperature. Mater Des 66:618–626
13. Karafillis AP, Boyce MC (1996) Tooling and binder design for sheet metal forming processes compensation springback error. Int J Mach Tools Manuf 36(4):503–536
14. Gan W, Wagoner RH (2004) Die design method for sheet springback. Int J Mech Sci 46:1097–1113
15. Anagnostou EL (2002) Optimized tooling design algorithm for sheet metal forming over reconfigurable compliant tooling. PhD thesis, State University of New York at Stony Brook
16. Cheng HS, Cao J, Xia ZC (2007) An accelerated springback compensation method. Int J Mech Sci 49(3):267–279
17. Wagoner RH, Gan W, Mao K, Price S, Rasouli F (2003) Design of sheet forming dies for springback compersation. Proceedings of ESAFORM 2003 7–14
18. Lingbeek R, Hu'etink J, Ohnimusb S, Petzoldt M, Weiher J (2005) The development of a finite elements based springback compensation tool for sheet metal products. J Mater Process Technol 169: 115–125
19. Cafuta G, Mole N, Stok B (2012) An enhanced displacement adjustment method: springback and thinning compensation. Mater Des 40:476–487
20. Mole N, Cafuta G, Stok B (2014) A 3D forming tool optimisation method considering springback and thinning compensation. J Mater Process Technol 214:1673–1685
21. Yang XA, Ruan F (2011) A die design method for springback compensation based on displacement adjustment. Int J Mech Sci 53:399–406